Australian Journal of Crop Science AJCS
AJCS 7(13):2079-2090 (2013) ISSN:1835-2707

Broken rice detection based on microwave measurement technique using microstrip wide-ring sensor and microstrip coupled-line sensor

Hou Kit Mun[1], Kok Yeow You[1*] and Mohamad Ngasri Dimon[1]

[1]Faculty of Electrical Engineering, Universiti Teknologi Malaysia, 81310 UTM, Skudai, Malaysia

***Corresponding author: kyyou@fke.utm.my**

Abstract

This paper proposes a microstrip wide-ring sensor and a microstrip coupled-line sensor for measuring the percentage of broken rice (BR) based on microwave measurement technique. Sensors with low insertion loss were developed to operate within a frequency range from 1 GHz to 3 GHz. The variations in percentage of BR with magnitude and phase of transmission coefficient were investigated using regression analysis at selected frequencies. Calibration equations for the measurement of the percentage of BR have been obtained and validated with white rice for percentage of BR ranging from 0% to 100%. The coupled-line sensor exhibits higher sensitivity to BR detection as compared with the wide-ring sensor. For a 1% change in BR, the change of phase for a coupled-line sensor is 0.00471 rad, around 20% of BR at 2.28 GHz. However, the change of phase for a wide-ring sensor with 1% change in BR is 0.00154 rad, around 20% of BR at 2.50 GHz. Also, the wide-ring sensor has greater accuracy in BR prediction than the coupled-line sensor. The wide-ring sensor has been found to be best suited for BR detection via the phase of transmission coefficient measurement at 2.50 GHz with 2.32% average error within 0% to 20% of BR. The coupled-line sensor is best suited for BR prediction from 20% to 60% by means of the measured phase of transmission coefficient at 2.28 GHz with an average error of less than 9.7%.

Keywords: Broken rice; microstrip wide-ring; microstrip coupled-line; microwave technique; phase; transmission coefficient.
Abbreviations: BR–broken rice; SOLT–short-open-load-through; SMA–subminiature version a; $|T|$–magnitude of transmission coefficient; ϕ–phase of transmission coefficient.

Introduction

Rice (*Oryza sativa* L.) is the staple food for more than half of the world's population. The quality of rice can be determined by moisture content, shape, chalkiness, whiteness and the number of broken rice grains. The head rice yield (the weight percentage of head rice or whole rice grains) is one of the important criteria for milled rice quality determination. The head rice yield after complete milling is influenced by many factors including paddy husked ratio, moisture content of rice grains, devices used for milling and milling duration (Yadav and Jindal, 2008). As the weight percentage of broken rice (BR) for the milled rice increases, the head rice yield decreases accordingly, and the quality of milled rice is reduced. Rice grains are considered as broken when their size is less than three quarters of whole grains (USDA, 2009). Normally, BR grains have only half of the value of whole rice grains (Cnossen et al., 2003). Consumers always want the best quality of edible rice at a fair price; hence, determining the percentage of BR accurately is important to protect consumers from price and quality manipulation. Conventionally, farmers use a grain grader with a separator, which is large in size and expensive, as a means of separating broken from whole grains. Then, the percentage of BR is computed by dividing the mass of broken grains by the total grain mass. As a result, this method is time-consuming. To overcome this, some researchers have applied machine vision systems as an indirect method for BR detection (Lloyd et al., 2001; Yadav and Jindal, 2001). However, a machine vision system requires an expert to set it up, is expensive and is affected by external light conditions. Other researchers have applied flatbed scanning and image analysis combined with a personal computer for rice breakage measurement (Van Dalen, 2004; Courtois et al., 2010). However, the specially designed software algorithm for this method is complex, especially with respect to image analysis. To the best of authors' knowledge, there are limited studies on the microwave technique for BR measurement. Recently, only You et al. (2011) have applied cylindrical slot antennas for BR measurement by means of the microwave technique; however, the device is relatively large in size and operates at a relatively high frequency (13.5 GHz), which increases the cost. Also, the microwave technique has also been applied for the moisture content determination of palm oil fruit (You et al., 2010a), hevea latex (Ansarudin et al., 2012), and *Dioscorea hispida* tubers (Zainuddin et al., 2013). Among the microwave techniques, the microstrip ring offers many advantages, such as; non-destructive measurement, easy sample loading and unloading when compared with the waveguide resonant cavity technique (Joshi et al., 1997), easy fabrication into a field portable device (Sarabandi and Li, 1997), no end effect compared to a single line resonator (Chang and Hsieh, 2004), maximum transmitted power as compared with a rejection filter (Sumesh Sofin and Aiyer, 2005) and accurate measurement in a dusty environment (Karazewski, 1998). Motivated by these advantages, the microstrip ring is used in this research. However, a typical microstrip ring with loose coupling will exhibit a high insertion loss of about 10 dB at the resonant frequency (Chang and Hsieh, 2004). When a signal is transmitted through the microstrip ring with high insertion loss, the transmitted signal will become very low.

Table 1. Dielectric properties for rice samples with different percentages of broken rice.

Percentage of BR (%)	0	20	40	60	80	100
ε_r'	2.2022	2.2537	2.3013	2.4394	2.4601	2.5133
ε_r''	0.2264	0.2515	0.2562	0.2851	0.2915	0.3126

Because of this very low transmission signal, some of the low cost measurement devices are unable to detect the transmitted signal. For this reason, this research has designed a microstrip ring sensor that exhibits low insertion loss at the resonant frequency. A microstrip coupled-line has been widely used in the filter application. It can be employed as a bandpass filter with low insertion loss and can be easily designed at any desired centre frequency. Besides this, it offers an attractive physical dimension that is small in size, light in weight and easy to fabricate. Although a microstrip coupled-line exhibits many advantages, it has not been applied to the determination of the percentage of BR. This paper proposes microstrip wide-ring and microstrip coupled-line sensors, which are designed to operate within a frequency range from 1 GHz to 3 GHz and exhibit low insertion loss for the percentage of broken rice grain determination. Both sensors operate at a relatively low frequency, within 1 GHz to 3 GHz, which can reduce the cost when compared with other devices that operate at a higher frequency. The microstrip ring is designed to have a wide ring in order to provide a relatively large contact area with the rice grains. Also, the 50 Ω feed lines are directly coupled with the ring to realize low insertion loss at the resonant frequency. Moreover, calibration equations for both sensors at selected frequencies are developed based on the relationship between the percentage of BR with corresponding measured magnitude and phase of transmission coefficient.

Results and Discussion

Simulation and measurement of sensors tested on free space

Figs. 1 and 2 show the comparative results of the simulated and measured transmission coefficient tested on free space for wide-ring sensor and coupled-line sensor respectively. There are small deviations between the measurement and simulation results for both sensors. The measured magnitude of transmission coefficient $|T|$ is slightly lower than the simulated $|T|$. The difference is mainly due to the losses within the SMA ports of the sensors (You et al., 2010b). Besides, the measured phase of transmission coefficient ϕ shifted to a lower frequency compared with the simulated ϕ. This is caused by the effect of the SMA ports on the measurement (You and Mun, 2012). The SMA ports are also excluded in the simulation for both sensors. The SMA ports are excluded because the Microwave Office software (AWR) is unable to simulate the SMA ports (a limitation of the software). Both sensors exhibit low insertion loss at resonant frequency when tested on free space. The minimum insertion loss for wide-ring sensor is close to 0.67 dB or $|T|$ equal to 0.93, while the minimum insertion loss for a couple-line sensor is close to 1.81 dB or $|T|$ equal to 0.81.

Variation in transmission coefficient with frequency for various percentages of broken rice

Figs. 3 and 4 illustrate the transmission coefficient as a function of frequency corresponding to different BR percentages for a wide-ring sensor and a coupled-line sensor. Experimental results show that an increment of BR percentage will cause the resonance curve of the transmission coefficient to shift toward lower frequencies and the decrement of maximum $|T|$ accordingly. The resonant frequency shifts to lower frequencies with the increase of BR percentages indicating that the dielectric constant ε_r' of the sample also increases with the increment of BR percentages according to Eqs. 2 to 5. Table 1 shows that the measured ε_r' increases with the BR percentages. As is well known, the bulk rice sample is a mixing of air and rice grains. The porosity size is inversely proportional to the percentage of BR grains. However, the permittivity of rice grains is higher than air. For a bulk rice sample with high BR percentage, the air porosity is lower, so the effective permittivity ε_{eff} of the overall bulk rice grain becomes higher (a high ε_{eff} indicates a high ε_r'). The increment of ε_r' will increase the ε_{eff} and hence the resonant frequency shifts toward lower frequencies (refer to Eqs. 2 to 5). The higher the ε_{eff} of bulk rice grain, the resonant frequency will shift to a lower frequency. The degree of shifting is affected by the percentage of BR. Besides, the decrement of $|T|$ is due to the increment of transmission loss (Nyfors and Vainikainen, 1989) when the BR percentage is increased. The loss in the transmission measurement is mainly caused by the rice grains rather than the air gap porosity in the bulk sample. When the percentage of BR is increased, the density of the rice grain will be increased in the bulk sample, and this will directly increase the transmission loss in the measurement. Moreover, the curve for ϕ also exhibits the tendency to shift to lower frequencies when the percentage of BR is increased. The increase of BR percentage will increase the ε_r' of the bulk rice sample, which will reduce the propagation speed of the transmitted wave leading to the ϕ to shift to lower frequencies.The results obtained are consistent with the theory introduced by Nyfors and Vainikainen (1989), where the change in relative permittivity ε_r of the materials (samples with different BR percentages have a different value of ε_r) will change the resonant frequency, ϕ and the insertion loss or $|T|$ for the probing microwaves. The change in ε_r of the materials will change the guided wavelength of transmitted frequency in the sample within the sensor. Since the resonant frequency is determined by the guided wavelength, the resonant frequency will be changed as a consequence. The degree of shifting for both $|T|$ and ϕ for a coupled-line sensor is higher when compared with a wide-ring sensor. This implies that the coupled-line sensor is more sensitive than the wide-ring sensor in BR detection. This is due to the coupled-line gap of the sensor being very sensitive to the BR that is contained within the gap. The microwave field lines within the coupled-line gap will act as a capacitance that is sensitive to the BR within the gap. The measured $|T|$ and ϕ corresponding to the percentage of BR range from 0% to 100% can be differentiated clearly within the sensitive frequency range of both sensors. For the wide-ring sensor, $|T|$ increases gradually as the BR percentage increases within the frequency range from 1.80 GHz to 2.28 GHz but reverses from 2.38 GHz to 2.52 GHz, while ϕ decreases with the increase in percentage of BR in the frequency range of 1.80 GHz to 2.60 GHz (Fig. 3). For the coupled-line sensor, $|T|$ increases gradually with the increase of BR percentage within the frequency range from 1.80 GHz to 2.10 GHz but reverses from 2.16 GHz to 2.42 GHz, while ϕ decreases as the BR

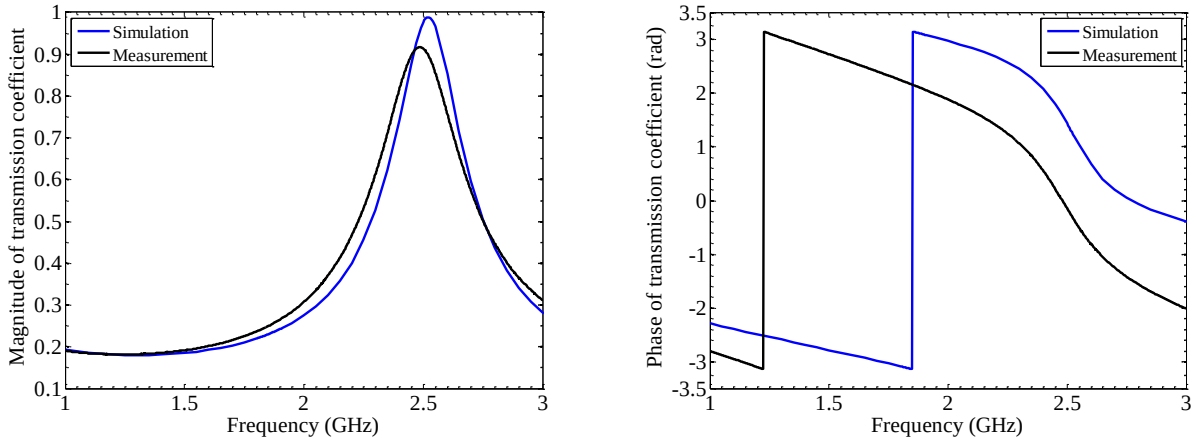

(a) (b)

Fig 1. Comparison between the variation in simulated and measured (a) magnitude and (b) phase of transmission coefficient with frequency for the wide-ring sensor tested with air. The simulation results were obtained from the AWR simulator while the measurements were carried out by using an E5071C Network Analyzer.

percentage increases within the frequency range of 1.80 GHz to 2.10 GHz but reverses from 2.20 GHz to 2.42 GHz (Fig. 4). The increment and decrement of |T| along the frequency range from 1 GHz to 3 GHz is due to the shifting and broadening of the resonance curve. In addition, the change in resonant frequency due to the change in BR percentage from 0% to 100% is located within the frequency range around 2.36 GHz to 2.38 GHz and 2.10 GHz to 2.16 GHz for the wide-ring sensor and the coupled-line sensor respectively.

Variation in percentage of broken rice with magnitude and phase of transmission coefficient at selected frequencies

A regression analysis was performed to determine the calibration equations and correlation between the BR percentages with corresponding $|T|$ and ϕ at selected frequencies for both sensors. The selection of frequency was determined by the largest changing rate of the $|T|$ and ϕ with respect to frequency within the sensitive frequency range. The sensitive frequency range for a wide-ring sensor is within 1.80 GHz to 2.28 GHz and 2.38 GHz to 2.52 GHz. Also, the sensitive frequency range for a coupled-line sensor is within 1.80 GHz to 2.10 GHz and 2.20 GHz to 2.42 GHz. Figs. 5 and 6 show the calibration curves relating the different percentages of BR with corresponding $|T|$ and ϕ at 1.93 GHz and 2.50 GHz for a wide-ring sensor. The calibration curves relating the different percentages of BR with the corresponding $|T|$ and ϕ at 1.83 GHz and 2.28 GHz for a coupled-line sensor are illustrated in Fig. 7 and 8. All the calibration equations based on the relationship between the percentage of BR with $|T|$ and ϕ at different frequencies were developed with 18 different rice samples over 0% to 100% of BR using regression analysis. The calibration equations and the corresponding coefficient of determination R^2 are given in Table 2. All the calibration equations for both sensors are in quadratic form. For a wide-ring sensor, the correlation between the percentage of BR and $|T|$ at 1.93 GHz is stronger than 2.50 GHz, based on higher R^2 of 0.8288. In contrast, the correlation between the percentage of BR and ϕ at 2.50 GHz is stronger than 1.93 GHz, based on a higher R^2 of 0.8740. This might be due to the $|T|$ at 1.93 GHz and ϕ at 2.50 GHz is less affected by the volume scattering of wave and multiple reflections compared with $|T|$ at 2.50 GHz and ϕ at 1.93 GHz respectively for the wide-ring sensor. For a coupled-line sensor, the correlation between the percentage of BR and $|T|$ at 2.28 GHz is stronger than 1.83 GHz, based on a higher R^2 of 0.8716. Also, the correlation between the percentage of BR and ϕ at 2.28 GHz is stronger than 1.83 GHz, based on higher R^2 of 0.8297. This might also be due to the $|T|$ and ϕ at 2.28 GHz is less affected by the volume scattering of wave and multiple reflections compared with $|T|$ and ϕ at 1.83 GHz for the coupled-line sensor. In this study, the porosity structure of the bulk rice sample is assumed to be uniformly distributed when the rice grain is poured into the sensor holder. For this reason, the unconsidered random porosity structure in the bulk rice will contribute to the uncertainty of the measurement. This can be improved by averaging the measured value of the same sample with repeated measurements.

The performance characteristics of the sensors

The average margin of error and degree of sensitivity of wide-ring and coupled-line sensors were determined in order to examine the performance of the sensors at selected frequencies. The sensitivity equations for both sensors are given in Table 3. Fig. 9 shows the comparative variation in sensitivity in absolute form with the percentage of BR based on measured $|T|$ and ϕ at selected frequencies for both sensors. The sensitivity of a wide-ring sensor based on measured $|T|$ at 2.50 GHz is higher than 1.93 GHz for BR ranging from 0% to 100%, while the sensitivity of the sensor based on measured ϕ at 2.50 GHz is higher than 1.93 GHz for BR ranging from 0% to 91%. In general, the sensitivity of the wide-ring sensor initially shows the trend to decrease with percentage of BR, and then the trend of slightly increasing occurs within the very high percentage range of BR. The coupled-line sensor exhibits greater sensitivity based on measured $|T|$ at 2.28 GHz than 1.83 GHz for BR ranging from 0% to 100%, while the sensitivity of the sensor based on measured ϕ at 2.28 GHz is higher than 1.83 GHz for BR ranging from 0% to 86%. In general, the sensitivity of the coupled-line sensor decreases with the rise in BR percentage. This might be due to the fact that the increment of BR percentage makes the sensing area of the coupled-line sensor more likely to be fully occupied by the BR, with the consequence that the sensitivity is reduced. Overall, the coupled-line sensor exhibits the highest sensitivity in BR prediction via $|T|$ and ϕ measurement at 2.28 GHz. For 1% change in percentage of BR, the change of ϕ for the coupled-

Table 2. Calibration equation relating percentage of broken rice with the magnitude and phase of transmission coefficient for the wide-ring and coupled-line sensors at different frequencies.

Sensor	Measured parameter	Frequency (GHz)	Calibration equation	R^2
Wide-ring	$\|T\|$	1.93	$BR = 119781.53452\|T\|^2 - 75620.06268\|T\| + 11911.59888$	0.8288
		2.50	$BR = 14451.77159\|T\|^2 - 24678.18077\|T\| + 10283.96782$	0.7400
	ϕ	1.93	$BR = 7873.94165\phi^2 - 29444.11854\phi + 27510.22726$	0.8028
		2.50	$BR = 5479.77309\phi^2 + 7234.81986\phi + 2382.18976$	0.8740
Coupled-line	$\|T\|$	1.83	$BR = -167036.98880\|T\|^2 + 20487.42279\|T\| - 510.40676$	0.6244
		2.28	$BR = 24955.81662\|T\|^2 - 6277.34250\|T\| + 381.97929$	0.8716
	ϕ	1.83	$BR = -902.75475\phi^2 + 704.40121\phi - 31.07822$	0.7343
		2.28	$BR = 150.90069\phi^2 - 635.19162\phi + 575.22941$	0.8297

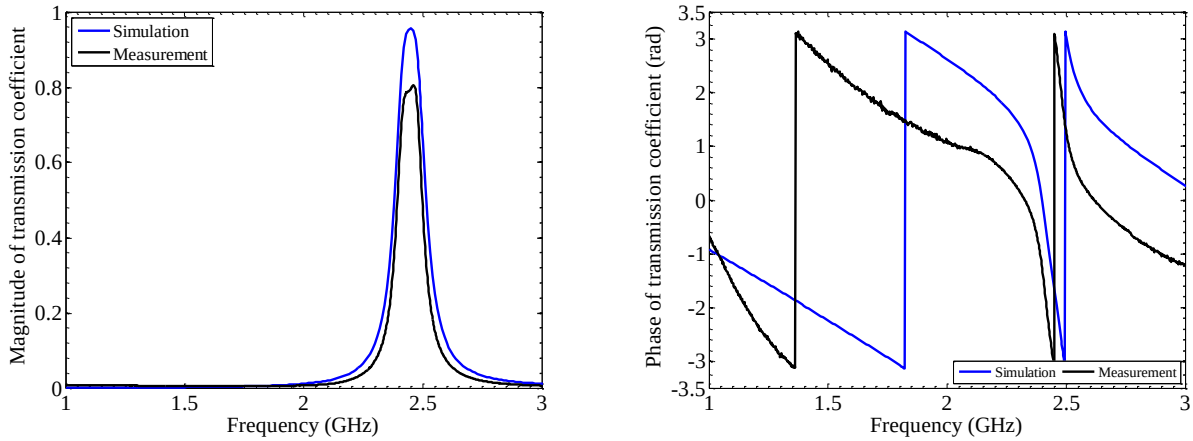

(a) (b)

Fig 2. Comparison between the variation in simulated and measured (a) magnitude and (b) phase of transmission coefficient with frequency for the coupled-line sensor tested with air. The simulation results were obtained from the AWR simulator while the measurements were carried out by using an E5071C Network Analyzer.

line sensor is 0.00471 rad, around 20% of BR at 2.28 GHz. For the wide ring sensor, the change of ϕ for 1% change in BR percentage is 0.00154 rad, around 20% of BR at 2.50 GHz. The sensors can be used practically, since the ϕ changes, resulting from 1% change in BR percentage, are more than the phase resolution (0.00034 rad) of the network analyzer. Twelve additional different rice samples over 0% to 100% of BR were prepared to validate the calibration equations. The predicted percentages of BR calculated from calibration equations were plotted against the actual percentage of BR determined from Eq. 1 as the solid line representing the ideal fit (Figs. 10 and 11). The summaries of validation results for both sensors are presented in Table 4. The average error is found by averaging the absolute errors between the predicted percentage of BR and the actual percentage of BR. For the wide-ring sensor, the R^2 and average error in percentage of BR prediction based on measured $|T|$ for calibration equation at 1.93 GHz are 0.8775 and 9.66% respectively, while for the calibration equation at 2.50 GHz they are 0.6520 and 16.20% respectively. Also, the R^2 and average error in prediction based on measured ϕ for calibration equation at 1.93 GHz are 0.8897 and 9.07% respectively, while for the calibration equation at 2.50 GHz are 0.8837 and 8.97% respectively. A high R^2 value indicates that the correlation between the predicted and actual BR percentage is good. The lowest average error is located at 2.50 GHz by means of a ϕ measurement for the wide-ring sensor. For the coupled-line sensor, the R^2 and average error in percentage of BR prediction based on measured $|T|$ for calibration equation at 1.83 GHz are 0.7016 and 15.41% respectively, while for the calibration equation at 2.28 GHz are 0.8654 and 10.84% respectively. Moreover, the R^2 and average error in prediction based on measured ϕ for calibration equation at 1.83 GHz are 0.7248 and 16.51% respectively, while for the calibration equation at 2.28 GHz they are 0.8886 and 9.88% respectively. The lowest average error is located at 2.28 GHz by means of a ϕ measurement for the coupled-line sensor. Overall, the wide-ring sensor is suitable for percentage of BR measurement from 0% to 100% at 2.50 GHz with average error of about 8.97 % via ϕ measurement, while the coupled-line sensor is suitable for BR detection at 2.28 GHz with average error of about 9.88% via ϕ measurement. This indicates that the wide-ring sensor shows higher accuracy than the coupled-line sensor in BR prediction. Both sensors show higher accuracy in BR detection based on ϕ measurement compared with $|T|$ measurement. This could be due to the fact that the inhomogeneous material (broken rice) will cause the volume scattering of wave and multiple reflections, which consequently give an erroneous $|T|$ measurement. However, the ϕ shift is less affected by the multiple reflections and the volume scattering of wave due to the grain size distribution compared with attenuation (Nyfors and Vainikainen, 1989). The results obtained in this study are consistent with other reports such

Table 3. Sensitivity equation for the wide-ring and coupled-line sensors at different frequencies.

Sensor	Measured parameter	Frequency (GHz)	Sensitivity equation
Wide-ring	$\|T\|$	1.93	$\frac{d\|T\|}{dBR} = -3.41193\times10^{-6}\,BR + 3.23415\times10^{-4}$
		2.50	$\frac{d\|T\|}{dBR} = 3.11006\times10^{-6}\,BR - 3.34783\times10^{-4}$
	ϕ	1.93	$\frac{d\phi}{dBR} = 1.69927\times10^{-5}\,BR - 1.48072\times10^{-3}$
		2.50	$\frac{d\phi}{dBR} = 2.02581\times10^{-5}\,BR - 1.94436\times10^{-3}$
Coupled-line	$\|T\|$	1.83	$\frac{d\|T\|}{dBR} = -1.14204\times10^{-6}\,BR + 1.49895\times10^{-4}$
		2.28	$\frac{d\|T\|}{dBR} = 4.15943\times10^{-6}\,BR - 5.86580\times10^{-4}$
	ϕ	1.83	$\frac{d\phi}{dBR} = 2.54997\times10^{-5}\,BR - 2.92246\times10^{-3}$
		2.28	$\frac{d\phi}{dBR} = 5.99154\times10^{-5}\,BR - 5.90598\times10^{-3}$

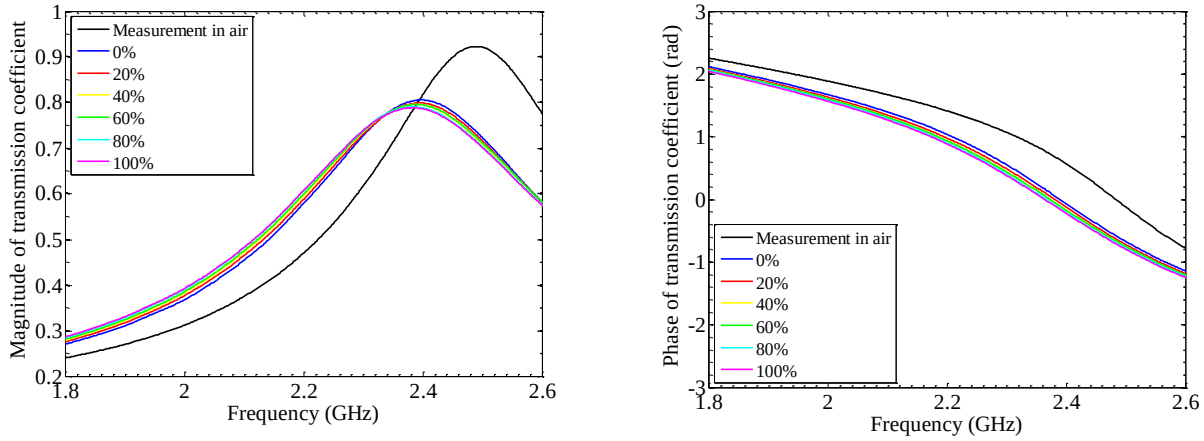

(a) (b)

Fig 3. Variation in (a) magnitude and (b) phase of transmission coefficient with frequency corresponding to different percentages of broken rice for the wide-ring sensor. The percentages of broken rice range from 0% to 100%.

as the measurement of moisture content in palm oil fruits (You et al., 2010a) and hevea rubber latex (Ansarudin et al., 2012), which also have shown better performance by using phase compared with magnitude of reflection coefficient $|\Gamma|$. Fig. 12 presents the variation in average errors corresponding to different percentages of BR for both sensors by means of the transmission coefficient measurement at selected frequencies. According to the error analysis, the wide-ring sensor is best suited for percentage of BR prediction from 0% to 40% at 2.50 GHz, with an average error rate of less than 6.8% via ϕ measurement. Moreover, the ring sensor can achieve an average error of about 2.32% for BR detection from 0% to 20% at 2.50 GHz via ϕ measurement. On the other hand, the coupled-line sensor is best suited for BR detection from 20% to 60% at 2.28 GHz with an average error rate of less than 9.7% by means of ϕ measurement. In practice, the percentage of BR may vary from as low as 5% to as high as 60% depending on the milling conditions. Normally, the quality of milled rice can be classified into four grades according to the percentage of BR, which are Premium (0% - 5%), Grade 1 (5% – 20%), Grade 2 (20% – 35%) and Grade 3 (35% – 50%). A comparison of proposed sensors with previous methods is presented in Table 5. The wide-ring sensor shows the average error of about 2.32 % for 0% to 20% BR prediction, which is comparable to the image analysis method proposed by Van Dalen (2004) for BR detection from 0% to 25% with a 2% average error. The coupled-line sensor exhibits a higher average error when compared with other devices. However, the average error of the coupled-line sensor is lower than the conventional method (Grain grader with separator), which has an average error of about 15%. The high error of the grader is caused by imprecise separation of whole and broken grain during the separation process (Yadav and Jindal, 2001). So, the coupled-line sensor can be an alternative to the conventional method for predicting the BR percentage. Moreover, the error of the proposed sensors can be further reduced by averaging the predicted BR percentages of the same sample with repeated measurements. The overall results obtained from this study suggest that the proposed sensors can be used as alternative methods for rapid BR percentage detection, having the advantages of smaller size, simpler and lower costs than previous methods such as machine vision systems (Lloyd et al., 2001; Yadav and Jindal, 2001), flatbed scanning and image analysis (Van Dalen, 2004; Courtois et al., 2010), and cylindrical slot antennas (You et al., 2011). In addition, the

Table 4. Summary of validation results for the wide-ring and coupled-line sensors.

Sensor	Measured parameter	Frequency (GHz)	Average error (%)	R^2
Wide-ring	$\|T\|$	1.93	9.66	0.8775
		2.50	16.20	0.6520
	ϕ	1.93	9.07	0.8897
		2.50	8.97	0.8837
Coupled-line	$\|T\|$	1.83	15.41	0.7016
		2.28	10.84	0.8654
	ϕ	1.83	16.51	0.7248
		2.28	9.88	0.8886

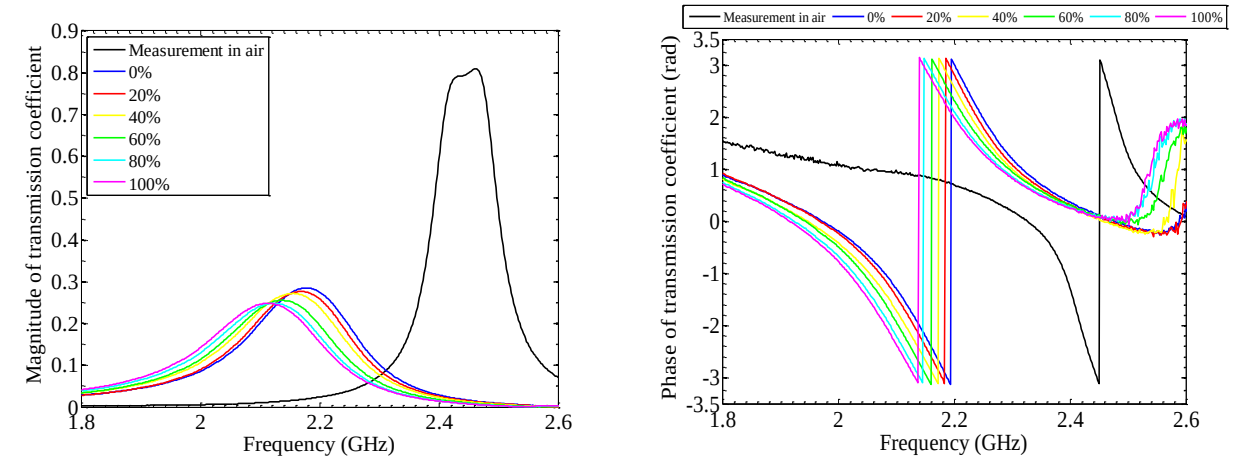

Fig 4. Variation in (a) magnitude and (b) phase of transmission coefficient with frequency corresponding to different percentages of broken rice for the coupled-line sensor. The percentages of broken rice range from 0% to 100%.

proposed sensors used in this study can predict the BR percentages from 0% to 100% when compared with the image analysis method used by Van Dalen (2004), which can only determine the percentages of BR between 0% and 25%.

Materials and methods

Fabrication of sensor

The microstrip wide-ring and the coupled-line sensors have been designed using Microwave Office software (AWR) in order to operate within the microwave frequency range from 1 GHz to 3 GHz, where their resonant frequencies are located at 2.49 GHz and 2.45 GHz respectively. All sensors were fabricated on RT/Duroid 5880 substrate. The dimensions of the sensors have been sketched by using AutoCAD software and printed on transparent paper, then delineated on the substrate by standard photolithography and etching. Then, both sensors were held on an aluminum ground with two SubMiniature version A (SMA) connectors, which allowed the sensors to be connected to the ports of an Agilent E5071C Network Analyzer. Finally, the sensors were covered with an acrylic holder (Fig. 13). Fig. 14 shows the configuration and dimensions of the wide-ring sensor and coupled-line sensor. The specifications of the RT/Duroid 5880 substrate and dimensions of the sensors are tabulated in Tables 6 and 7.

Grain sample preparation and measurement

Jati™ *Indica* species long grain white rice, which is grown in the fertile soil of Kedah, the Rice Bowl of Malaysia, was used as the experimental sample. The average length, width and moisture content (wet basis) of the rice grain are 7.10 mm, 2.04 mm and 14% respectively. The broken grains were obtained by being specially broken with a blender. Rice grain samples with different percentages of BR were prepared by mixing broken and whole grains. The percentage of BR was determined as the ratio (in percentage) of the mass of the broken grains over the total mass of the sample (whole and broken) which is expressed as:

$$BR(\%) = \frac{m_{br}}{m_s} \times 100 \quad (1)$$

where m_{br} and m_s are the mass of broken grains and mass of sample respectively. The rice samples had percentages of BR ranging from 0% to 100% with 100 g per sample. Each of the samples was sealed in a different container before the measurements. A full two-port short-open-load-through (SOLT) calibration was performed at the 50 Ω coaxial cable of the network analyzer before being connected to the sensor. After the calibration, grain samples with different percentages of BR were placed into the sample holder of the sensor. The $|T|$ and ϕ corresponding to different samples were obtained from the network analyzer (Fig. 15). Also, the dielectric properties (dielectric constant ε_r' and loss factor ε_r'') of rice samples were measured by using an Agilent 85070E Dielectric Probe. The average value of the dielectric

Table 5. Comparison of previous methods for percentage of broken rice measurement.

Method	BR (%)	Average Error (%)	Cost	Size	Complexity	Set-up speed
Flatbed scanning and image analysis (Courtois et al., 2010)	0-90	2	Moderate	Medium	Complex	Fast
Flatbed scanning and image analysis (Van Dalen, 2004)	0-25	2	Moderate	Medium	Complex	Fast
Machine vision system (Lloyd et al., 2001)	0-100	2	High	Large	Complex	Moderate
Machine vision system (Yadav and Jindal, 2001)	0-100	1.2	High	Large	Complex	Moderate
Cylindrical slot antennas (You et al., 2011)	0-100	unknown	Low	Medium	Simple	Fast
Grain grader with separator (Conventional)	0-100	15	High	Large	Moderate	Slow
Wide-ring sensor (This study)	0-20	2.32	Low	Small	Simple	Fast
	0-40	3.79				
	0-100	8.97				
Coupled-line sensor (This study)	0-20	9.57	Low	Small	Simple	Fast
	0-40	9.59				
	0-100	9.88				

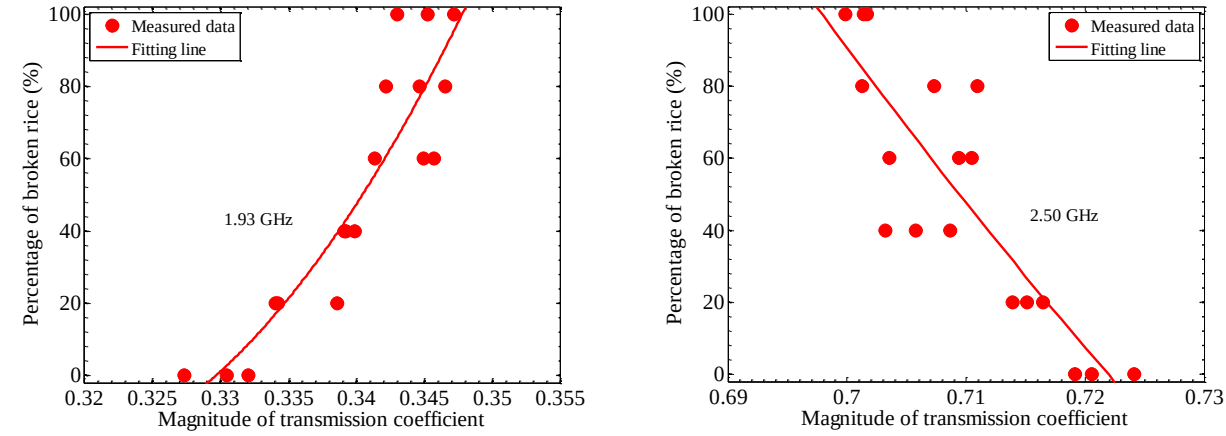

(a) (b)

Fig 5. Variation in percentage of broken rice with magnitude of transmission coefficient at (a) 1.93 GHz and (b) 2.50 GHz for the wide-ring sensor. The fitting lines represent the calibration curves for the calibration equations.

properties was obtained from fifteen repeated measurements of each sample. The average values of the dielectric properties for various percentages of BR at 2.42 GHz are tabulated in Table 1.

Regression analysis

The regression analysis was performed by using MATLAB software to determine the relationship between percentages of BR and the measured transmission coefficient at different frequencies. By using the "polyfit" function inside the MATLAB, different percentages of BR were fitted with the corresponding measured $|T|$ and ϕ in order to obtain the polynomial calibration equations. All the calibration equations for both sensors were developed with 18 different rice samples between 0% and 100% of BR (6 group of samples with 3 samples for each group). In addition, the R^2 value for all calibration equations, whose values were used to evaluate the fitting performance and to determine the correlation between the BR percentages with corresponding measured $|T|$ and ϕ, are also given in this analysis.

Principle and theory

In free space, the particular resonant frequency for a microstrip ring depends mainly on the effective permittivity ε_{eff} and the mean circumference of the conductor ring. The resonant frequency of the ring sensor can be approximated by

$$f_r = \frac{nc}{2\pi r\sqrt{\varepsilon_{eff}}} \quad (2)$$

where r is the mean radius of the ring, c is the speed of light, and n is the mode number.

Table 6. Substrate specifications and dimensions for the wide-ring sensor.

Substrate specifications	Dimension (mm)				
	W_r	W_f	R_i	R_o	l
$\varepsilon_{r,sub} = 2.2$ tan δ = 0.001 h = 0.381 mm	9.03	1.14	8.92	17.96	11.09

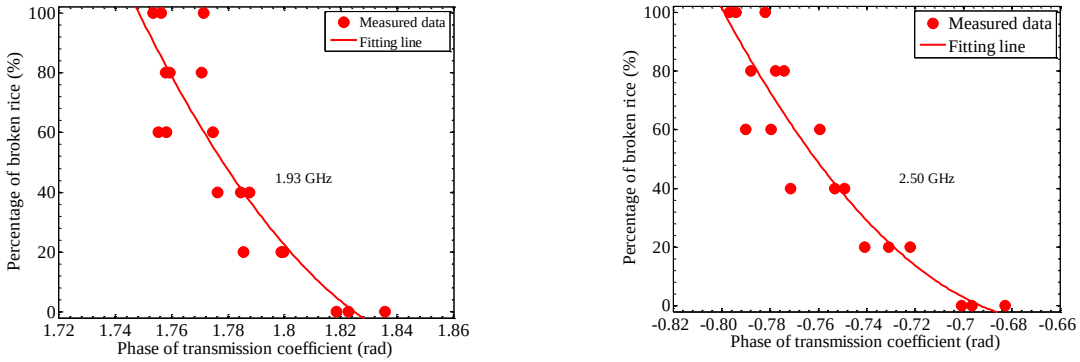

(a) (b)

Fig 6. Variation in percentage of broken rice with phase of transmission coefficient at (a) 1.93 GHz and (b) 2.50 GHz for the wide-ring sensor. The fitting lines represent the calibration curves for the calibration equations.

Table 7. Substrate specifications and dimensions for the coupled-line sensor.

Substrate specifications	Dimension (mm)							
	L_1	L_2	L_3	W_1	W_2	W_3	S_1	S_2
$\varepsilon_{r,sub} = 2.2$ tan δ = 0.001 h = 0.787 mm	22.3	22.1	22.0	2.4	2.0	2.3	0.3	2.0

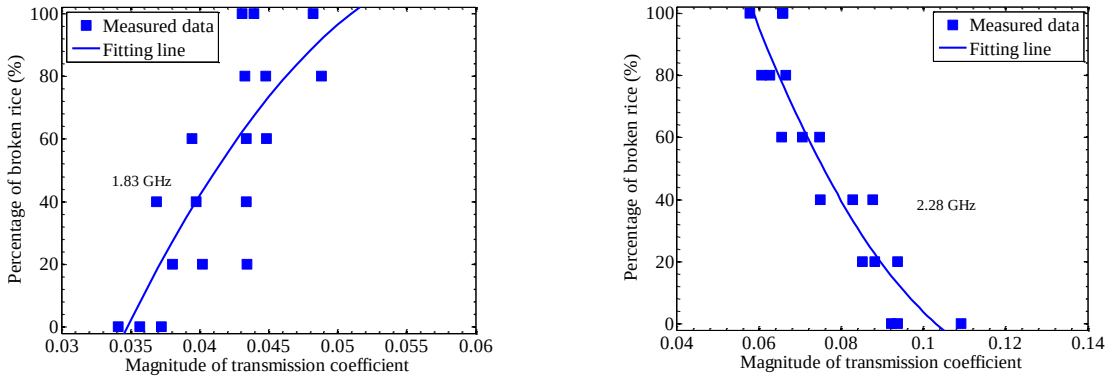

(a) (b)

Fig 7. Variation in percentage of broken rice with magnitude of transmission coefficient at (a) 1.83 GHz and (b) 2.28 GHz for the coupled-line sensor. The fitting lines represent the calibration curves for the calibration equations.

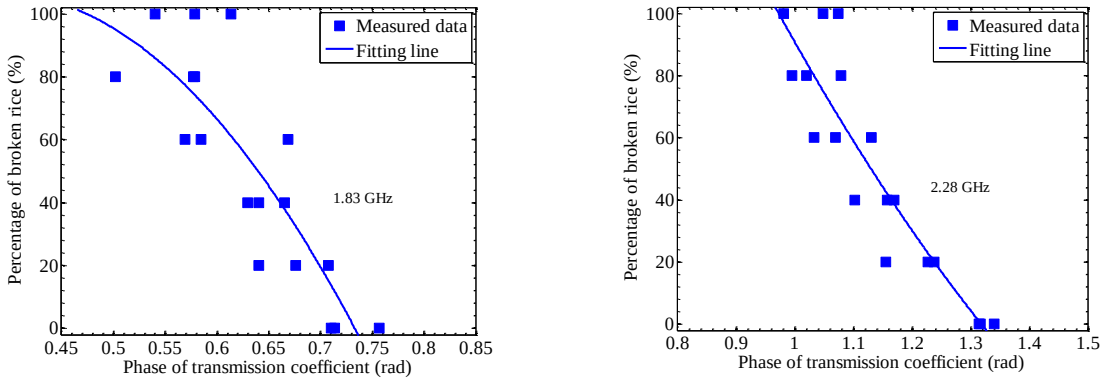

(a) (b)

Fig 8. Variation in percentage of broken rice with phase of transmission coefficient at (a) 1.83 GHz and (b) 2.28 GHz for the coupled-line sensor. The fitting lines represent the calibration curves for the calibration equations.

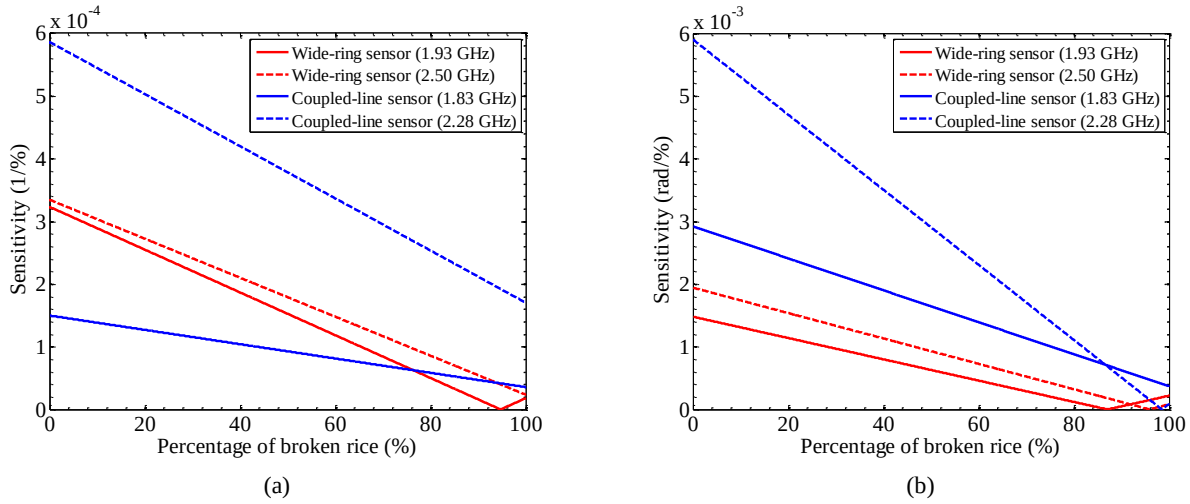

Fig 9. Variation of sensitivity in absolute form with percentage of broken rice based on the measured (a) magnitude and (b) phase of transmission coefficient for the wide-ring and coupled-line sensors. The plots suggest that the coupled-line sensor exhibits a higher sensitivity compared with the wide-ring sensor.

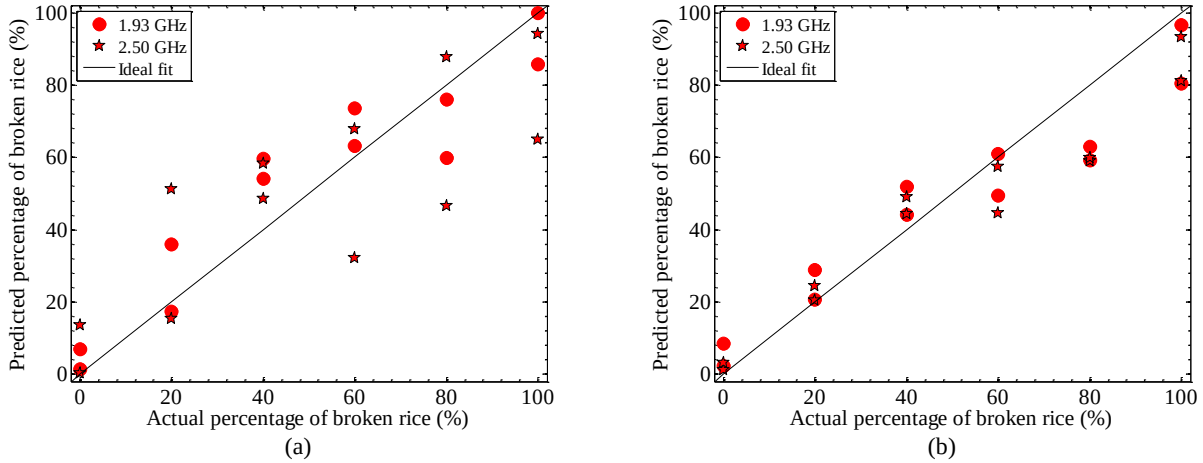

Fig 10. Comparison of the predicted and actual percentage of broken rice based on the measured (a) magnitude and (b) phase of transmission coefficient for the wide-ring sensor. The ideal fit represents the ideal relationship between predicted and actual percentage of broken rice.

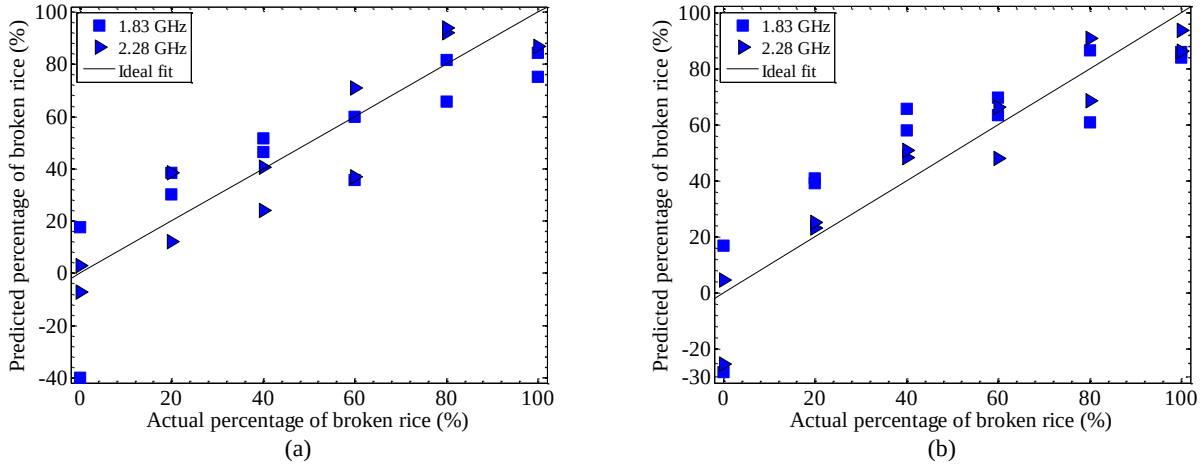

Fig 11. Comparison of the predicted and actual percentage of broken rice based on the measured (a) magnitude and (b) phase of transmission coefficient for the coupled-line sensor. The ideal fit represents the ideal relationship between predicted and actual percentage of broken rice.

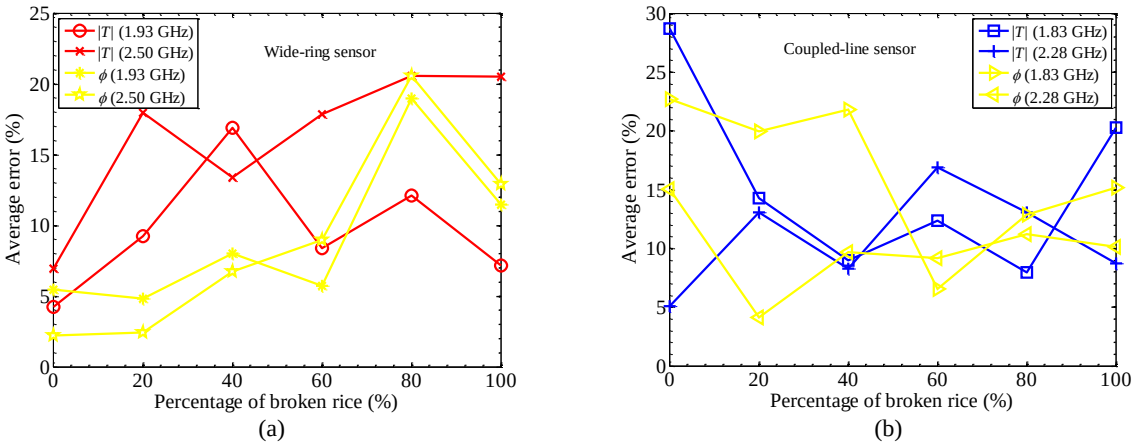

Fig 12. Variation of average error with percentage of broken rice for (a) the wide-ring sensor and (b) the coupled-line sensor. The plots suggest that the wide-ring sensor exhibits higher accuracy compared with the coupled-line sensor.

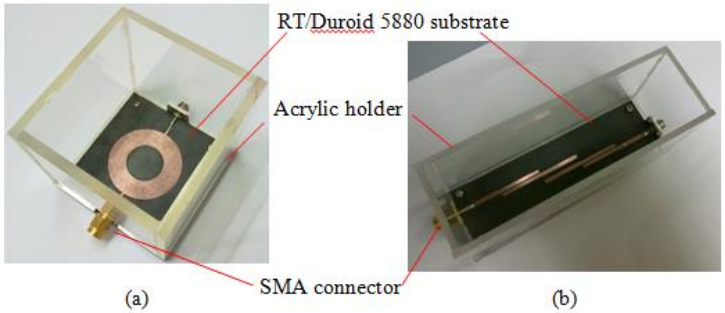

Fig 13. The designed sensors (a) wide-ring sensor (b) coupled-line sensor.

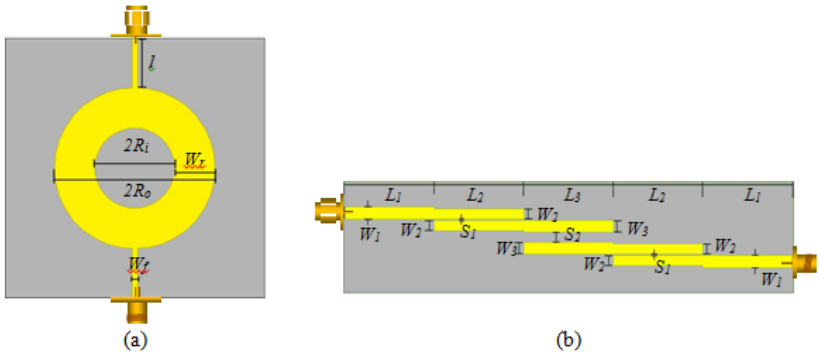

Fig 14. Configuration and dimensions of the sensors. (a) Wide-ring sensor with width of the ring W_r, width of the feed line W_f, length of the feed line l, inner radius of the ring R_i and outer radius of the ring R_o. (b) Coupled-line sensor with width of the line W_n, length of the line L_n and gap within the line S_n.

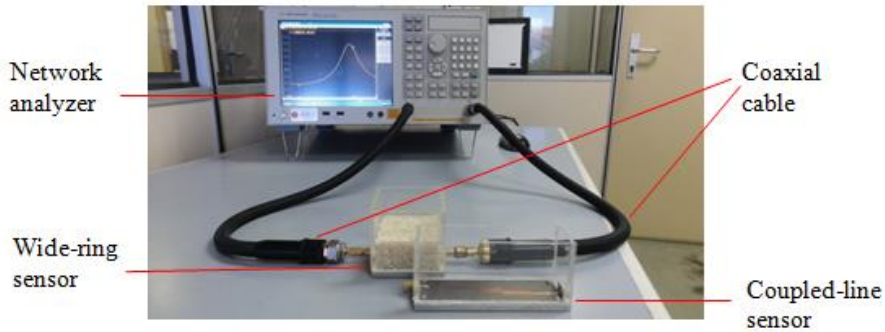

Fig. 15. Measurement set-up.

The ε_{eff} is evaluated as

$$\varepsilon_{eff} = \frac{\varepsilon_{r,sub} + \varepsilon_r'}{2} + \frac{\varepsilon_{r,sub} - \varepsilon_r'}{2}\left(1+12\frac{h}{W_r}\right)^{-0.5} \quad (3)$$

where $\varepsilon_{r,sub}$ is the dielectric constant of the substrate, W_r is the width of the ring, h is the substrate thickness, and ε_r' is the dielectric constant of the material that covers the ring sensor. When the ring sensor is fully filled with air, then ε_r' is equal to 1. Whereas, if the ring sensor is overlaid with rice grain, the ring sensor will produce a resonant frequency shift and a broadening of the resonance curve (a change in the transmission coefficient) when compared to free space. The ε_r' relates with the capability of energy storage in the electric field in the material (Nelson and Trabelsi, 2005). The percentage of BR within a bulk rice grain will affect the porosity of the bulk rice. The interaction of the microwave or electric field with the rice grain is influenced by the size of air gaps within the rice grain. Thus, rice grain with different percentages of BR will have a different value for ε_r'. When rice grain with various percentages of BR is placed on the ring sensor, the resonance curve will be changed accordingly. In this study, a wide ring was designed in order to have a relatively large contact area with the rice grains. The 50 Ω feed lines are coupled to the ring directly to realize low insertion loss and low radiation loss at the f_r. Consequently, the coupling effect will alleviate the f_r and Eq. 2 is modified as follow:

$$f_r = \chi\frac{nc}{2\pi r\sqrt{\varepsilon_{eff}}} \quad (4)$$

where χ is the correction factor. The value of χ is obtained from the measured f_r when the ring is tested with free space. The value of χ in this study is 1.0141. The coupled-line sensor design is based on Butterworth routine filter theory. For the sake of brevity, the detailed design of the sensor's physical dimensions can be referred to in several studies (Gupta et al., 1996; Mongia et al., 2007). After the coupled-line sensor was filled with rice grain having different percentages of BR, the sensor also exhibited a shift in its resonant frequency. The loaded (sensor in contact with the rice grains) resonant frequency of the coupled-line sensor can be determined as follow:

$$f_l = f_u - \frac{(\varepsilon_r' - 1) f_u}{2P} \quad (5)$$

where P is the filling factor and f_u represents the unloaded (sensor in contact with air) resonant frequency. The value of P was determined experimentally with a sample of known permittivity. The sample used in this study is corn oil with its permittivity obtained by using Agilent 85070E Dielectric Probe and E5071C Network Analyzer. The value of P was determined as 9.0087.

Conclusion

In this paper, a microstrip wide-ring and a microstrip coupled-line with low insertion loss have been presented as non-destructive sensors for determining the percentage of BR by means of the microwave measurement technique. Calibration equations for both sensors have been developed by using the relationship between the percentage of BR with measured magnitude and phase of transmission coefficients at selected frequencies. A comparative study of the performance characteristic of both sensors in BR detection has been made. The analysis shows that the sensitivity of the coupled-line sensor is higher than the wide-ring sensor, while the accuracy of the wide-ring sensor is higher than the coupled-line sensor. The validation tests have shown that the percentage of BR can be best predicted by a wide-ring sensor with an average error of 8.97% at 2.50 GHz via the phase of transmission coefficient measurement. On the other hand, the percentage of BR can be best predicted by a coupled-line sensor with an average error of 9.88% at 2.28 GHz by means of the measured phase of the transmission coefficient. For the best performance, a wide-ring sensor is more suited for percentage of BR prediction between 0% and 20% at 2.50 GHz with an average error of 2.3% via the phase measurement, while the coupled-line sensor is more suited for BR detection between 20% and 60% at 2.28 GHz with an average error of less than 9.7% by means of the phase measurement. The proposed sensors with their open structure and small size provide a simple, low-cost and non-destructive microwave measurement technique for the rapid determination of the percentage of BR. The proposed sensors are also suitable for determining the moisture content of other crops and agriculture products such as wheat, barley, oat and latex by recalibrating the sensors.

Acknowledgments

This work is financed by the Zamalah/Institutional Scholarship and Research University Grant (GUP) under project number Q.J130000.2623.05J55 provided by Universiti Teknologi Malaysia.

References

Ansarudin F, Abbas Z, Hassan J, Yahaya NZ, Ismail MA (2012) A simple insulated monopole sensor technique for determination of moisture content in hevea rubber latex. Meas Sci Rev 12(6): 249-254.

Chang K, Hsieh LH (2004) Microwave ring circuits and related structures, 2nd edn. John Wiley & Sons, Hoboken, New Jersey.

Cnossen AG, Jimenez MJ, Siebenmorgen TJ (2003) Rice fissuring response to high drying and tempering temperatures. J Food Eng 59: 61-69.

Courtois F, Faessel M, Bonazzi C (2010) Assessing breakage and cracks of parboiled rice kernels by image analysis techniques. Food Control 21: 567-572.

Gupta KC, Garg R, Bahl I, Bhartia P (1996) Microstrip lines and slotlines, 2nd edn. Artech House, Norwood, MA.

Joshi KK, Abegaonkar MP, Karekar RN, Aiyer RC (1997) Microstrip ring resonator as a moisture sensor for wheat grains. Paper presented at the IEEE MTT-S international microwave symposium, Denver, Colorado, USA, 8-13 June 1997.

Karazewski A (1998) Microwave aquametry - recent advances. Paper presented at the 3rd international symposium on humidity and moisture, London, England, 6-8 April 1998.

Lloyd BJ, Cnossen AG, Siebenmorgen TJ (2001) Evaluation of two methods for separating head rice from brokens for head rice yield determination. Appl Eng Agric 17(5): 643–648.

Mongia RK, Bahl IJ, Bhartia P, Hong J (2007) RF and microwave coupled-line circuits, 2nd edn. Artech House, Norwood, MA.

Nelson SO, Trabelsi S (2005) Permittivity measurements and agricultural applications. In: Kupfer K (ed) Electromagnetic aquametry. Springer, Berlin.

Nyfors E, Vainikainen P (1989) Industrial microwave sensors, Artech House, Norwood, MA.

Sarabandi K, Li ES (1997) Microstrip ring resonator for soil moisture measurements. IEEE Trans Geosci Remote Sens 35(5): 1223-1231.

Sumesh Sofin RG, Aiyer RC (2005) Measurement of dielectric constant using a microwave microstrip ring resonator (MMRR) at 10 GHz irrespective of the type of overlay. Microwave Opt Technol Lett 47(1): 11-14.

USDA (2009). United States standards for rice, 868.302 – definition of other terms. United States Department of Agriculture , Washington, DC.

Van Dalen G (2004) Determination of the size distribution and percentage of broken kernels of rice using flatbed scanning and image analysis. Food Res Int 37: 51-58.

Yadav BK, Jindal VK (2001) Monitoring milling quality of rice by image analysis. Comput Electron Agric 33(1): 19–33.

Yadav BK, Jindal VK (2008) Changes in head rice yield and whiteness during milling of rough rice (*Oryza sativa* L.). J Food Eng 86: 113-121.

You KY, Abbas Z, Khalid K (2010a) Application of microwave moisture sensor for determination of oil palm fruit ripeness. Meas Sci Rev 10(1): 7-14.

You KY, Mun HK (2012) Dielectric measurement using a planar ring sensor for low-loss powder form materials. Paper presented at the progress in electromagnetics research symposium, Kuala Lumpur, Malaysia, 27-30 March 2012.

You KY, Salleh J, Abbas Z, You LL (2010b) A rectangular patch antenna technique for the determination of moisture content in soil. Paper presented at the progress in electromagnetics research symposium, Cambridge, USA, 5-8 July 2010.

You KY, Salleh J, Abbas Z, You LL (2011) Cylindrical slot antennas for monitoring the quality of milled rice. Paper presented at the progress in electromagnetics research symposium, Suzhou, China, 12-16 September 2011.

Zainuddin MF, Abbas Z, Hafizi MHM, Jusoh MA, Razali MHH (2013) Monopole antenna technique for determining moisture content in the *Dioscorea hispida* tubers. Aust J Crop Sci 7(1): 1-6.